© 2016. Published by The Company of Biologists Ltd | Development (2016) 143, 1170-1181 doi:10.1242/dev.133165

RESEARCH ARTICLE

Drosophila astrocytes cover specific territories of the CNS neuropil and are instructed to differentiate by Prospero, a key effector of Notch

Emilie Peco[1,2], Sejal Davla[1,3], Darius Camp[1,4], Stephanie M. Stacey[1,3], Matthias Landgraf[5] and Don J. van Meyel[1,2,*]

ABSTRACT

Astrocytes are crucial in the formation, fine-tuning, function and plasticity of neural circuits in the central nervous system. However, important questions remain about the mechanisms instructing astrocyte cell fate. We have studied astrogenesis in the ventral nerve cord of *Drosophila* larvae, where astrocytes exhibit remarkable morphological and molecular similarities to those in mammals. We reveal the births of larval astrocytes from a multipotent glial lineage, their allocation to reproducible positions, and their deployment of ramified arbors to cover specific neuropil territories to form a stereotyped astroglial map. Finally, we unraveled a molecular pathway for astrocyte differentiation in which the Ets protein Pointed and the Notch signaling pathway are required for astrogenesis; however, only Notch is sufficient to direct non-astrocytic progenitors toward astrocytic fate. We found that Prospero is a key effector of Notch in this process. Our data identify an instructive astrogenic program that acts as a binary switch to distinguish astrocytes from other glial cells.

KEY WORDS: Astrocyte development, Astroglial map, Notch, Pointed, Prospero

INTRODUCTION

Astrocytes are among the most numerous cells in the mammalian central nervous system (CNS), with protoplasmic astrocytes projecting highly ramified arbors of infiltrative processes among neuronal cell bodies and synapses (Bushong et al., 2004; Distler et al., 1991; Ogata and Kosaka, 2002). Through extensive interactions with neurons, astrocytes employ a host of channels, receptors and transporters to maintain ion and neurotransmitter homeostasis, and modulate and respond to neuronal activity (Clarke and Barres, 2013). Individual astrocytes may coordinate these activities within their micro-anatomical domain, since astrocytes occupy exclusive territories with little or no overlap with their neighbors (Bushong et al., 2004; Distler et al., 1991; Halassa et al., 2007; Ogata and Kosaka, 2002). In addition, astrocytes appear tailored for precise roles at region-specific circuitry: within the developing mouse spinal cord, astrocytes are spatially restricted according to their region of origin (Hochstim et al., 2008; Tsai et al., 2012), providing local trophic support for neurons and spatially encoded information that influences the formation and refinement of neural circuits (Molofsky et al., 2014). Discovering the degree and precision with which astrocytes chart to specific CNS territories is a key step toward understanding how domain-specific astrocytes locally regulate neural circuit formation and function.

It is well appreciated that astrocytes emerge from complex interplay between cell-intrinsic programs and extrinsic influences such as secreted or contact-dependent signals from neurons (for reviews see Kanski et al., 2014; Molofsky et al., 2012). For example, newborn neurons in mammals stimulate astrogenesis in progenitor cells by secreting the cytokine cardiotrophin 1 (Barnabé-Heider et al., 2005) and by contact-mediated communication via the Notch signaling pathway (Namihira et al., 2009; Yoon et al., 2008). Notch effectors include the bHLH Hes factors, which inhibit neurogenesis and promote STAT3, a direct activator of astrocytic genes (Kamakura et al., 2004). Another Notch target, the nuclear factor NF1A, is crucial for initiating astrogenesis through demethylation of astrocytic gene promoters that can then be bound by STAT3 for transcriptional activation (Deneen et al., 2006). Despite recent progress, defining astrogenic pathways *in vivo* has been complicated by imperfect markers, and because astrocytes in mammals arise from multipotent progenitors that generate neurons first (Molofsky et al., 2012). For these reasons, we investigated astrogenesis *in vivo* using the *Drosophila* larva CNS, a relatively simple and genetically tractable model. The larval ventral nerve cord (VNC) has a defined number of identifiable glial cells (Beckervordersandforth et al., 2008). This allows the precise positioning and emergence of astrocytes to be followed in exquisite detail, a key advantage compared with mammalian model systems.

Like their mammalian counterparts, *Drosophila* astrocytes extend processes that infiltrate the synaptic neuropil, and tile with one another to occupy non-overlapping territories (Awasaki et al., 2008; Doherty et al., 2009; Omoto et al., 2015; Stork et al., 2014). *Drosophila* astrocytes respond to neuronal activity with altered transporter expression and intracellular calcium dynamics (Muthukumar et al., 2014; Stork et al., 2014), they influence CNS synapse number during neural circuit formation (Muthukumar et al., 2014) and modulate locomotor behavior, seizures and olfactory processing (Liu et al., 2014; Rival et al., 2004; Stacey et al., 2010; Stork et al., 2014). However, little is known about how *Drosophila* astrocytes are organized relative to specific regions of the synaptic neuropil, or of the key regulatory programs that govern the acquisition of astrocyte fate versus that of other glial cell types.

We report that larval astrocytes derive from a lineage that also gives rise to non-astroglial cells. Astrocytes are distinguished by their expression of the homeodomain transcription factor Prospero, known previously for its role in neuroblast lineages to halt stem cell

[1]Centre for Research in Neuroscience, Department of Neurology and Neurosurgery, McGill University, Montreal, Quebec, Canada H3G 1A4. [2]Research Institute of the McGill University Health Centre, Montreal, Quebec, Canada H3G 1A4. [3]McGill Integrated Program in Neuroscience McGill University, Montreal, Quebec, Canada H3A 2B4. [4]Division of Experimental Medicine, McGill University, Montreal, Quebec, Canada H3A 1A3. [5]Department of Zoology, University of Cambridge, Cambridge CB2 3EJ, UK.

*Author for correspondence (don.vanmeyel@mcgill.ca)

Received 19 November 2015; Accepted 8 February 2016

Development (2016) 143, 1170-1181 doi:10.1242/dev.133165

division and initiate neuronal differentiation (Choksi et al., 2006; Vaessin et al., 1991). We find that individual astrocytes are allocated to reproducible regions, and that their infiltrative arbors cover territories of the CNS neuropil that are remarkably stereotyped. Seeking factors essential for the differentiation of astrocytes, we find that Notch signaling is astrogenic, as it is in mammals, and that the Ets transcription factor Pointed is also required. However, only Notch signaling is sufficient to direct non-astrocyte progenitors toward astrocyte fate. We demonstrate that Prospero is a key effector of Notch in this process, identifying the Notch-Prospero program as a crucial switch that is both essential and instructive to engage astrocyte differentiation during development.

RESULTS

Longitudinal glia generate astrocytes, ensheathing and ensheathing/wrapping glia

Longitudinal glia (LG), which are exclusively derived from the longitudinal glioblast (LGB) (Beckervordersandforth et al., 2008; Schmid et al., 1999), are thought to be the embryonic precursors of larval astrocytes, but no systematic high-resolution analysis has mapped their mature identities and organization in first-instar larvae (L1). We resolved this using *AO75-lacZ* (Fig. 1A,B), a specific reporter for embryonic LG (Beckervordersandforth et al., 2008). As in embryos, we found it labeled nine cell bodies per hemisegment at the interface between neuropil and cortex that were confirmed to be LG by colabeling with *Nazgul-nGFP*, another LG reporter (Fig. 1A-C″) that also happens to be expressed in other glial cells such as cortex glia (Fig. 1B,B′, arrows) (Stacey et al., 2010). We then examined subtypes among LG (Fig. 1C-C‴, dashed circles) and found that, as in embryos, six of the nine LG express Prospero (Griffiths et al., 2007; Griffiths and Hidalgo, 2004; Ito et al., 1995). Of the remaining three that did not (Fig. 1C, arrowheads), one expressed *Salm-lacZ* (Fig. 1D-D‴, arrowheads), which in embryos marks the lateral posterior LG (LP-LG) (Beckervordersandforth et al., 2008).

We next assessed LG morphologies using the 'Blown-OUT' technique to visualize small clones of cells. Blown-OUT is akin to the Flp-OUT technique except that it employs B3 recombinase instead of Flp to achieve site-specific recombination of a reporter transgene (Nern et al., 2011). Using *Eaat1-Gal4* and *Nazgul-Gal4* (Table 1), clones ranging in size from one to eight cells were labeled with membrane-targeted RFP (myr-RFP). The only cell found in single-cell clones (Fig. 1G) did not express Prospero (Fig. 1G, inset), formed a sheath over the dorsal aspect of the neuropil and wrapped a proximal portion of the intersegmental nerve, giving it features of both ensheathing and wrapping glia. Among two-cell clones, 88% were pairs of Prospero$^+$ astrocytes extending infiltrative processes into the neuropil (Fig. 1E). The remaining 12% of two-cell clones did not express Prospero (Fig. 1F, inset) and were pairs of ensheathing glia enveloping the ventral and medial aspects of the neuropil between neuromeres (Fig. 1F). We confirmed that Prospero was not expressed in ensheathing and ensheathing/wrapping glia labeled with *R56C01-Gal4* (Table 1, Fig. 1H). These data confirm that the nine embryonic LG in each hemisegment become six larval astrocytes (Prospero$^+$), two ensheathing glia, and one glial cell with combined ensheathing/wrapping features that we deduced to be the LP-LG based on its dorsomedial position (as summarized in Fig. 1I).

Drosophila astrocytes infiltrate specific neuropil territories

To achieve a better understanding of astrocyte differentiation, the organization of astrocytes has to be characterized. Astrocyte cell bodies consistently occupied particular regions around the neuropil (Fig. 1I), comparable to their positions seen in third-instar larval VNC (Ito et al., 1995; Kato et al., 2011; Stork et al., 2014). Indeed, among the six astrocytes by hemisegment, three are at dorsal positions, two are more laterally located and one is ventral. More significantly, we discovered that astrocytes in two-cell clones were non-randomly paired since, based on the relative positions of their cell bodies, 90% could be classified into one of only three categories (Fig. 2A-D). Either both astrocytes in the pair were positioned dorsally (Cat.1 D/D, Fig. 2B), both astrocytes were positioned laterally (Cat.2 L/L, Fig. 2C), or one dorsal astrocyte was paired with the ventral astrocyte (Cat.3 D/V, Fig. 2D). Since astrocytes in two-cell clones are likely to be siblings, non-random pairings indicate that within each hemisegment there are three sibling pairs of astrocytes spatially allocated to distinct regions. In order to evaluate how precise their positions were within these regions (dorsal, lateral, ventral), we charted GFP-labeled nuclei in two-cell clones with respect to axon bundles labeled by Fas2 (Fig. 2E-G) (Landgraf et al., 2003b). These provide specific and consistent neuropil landmarks to map astrocytes along the dorsoventral and mediolateral axes (Fig. 2F) and the anteroposterior axis (Fig. 2G). Our results indicated that the cell bodies of astrocytes are clearly allocated to one of three distinct regions around the neuropil, yet within each region their positions were rather imprecise (Fig. 2F,G).

We then asked if the regional allocation of astrocyte cell bodies was accompanied by their coverage of specific zones of the neuropil. As in the nervous system of many organisms, the *Drosophila* VNC neuropil displays spatial segregation of functionally distinct regions: the dorsal neuropil harbors presynaptic terminals that converge onto motor neurons, whereas the ventral region contains synaptic inputs from sensory neurons (Grueber et al., 2007; Landgraf et al., 2003a; Merritt and Whitington, 1995; Zlatic et al., 2003). We systematically charted the territories covered by astrocyte arbors, mapping two-cell Blown-OUT clones arbors with respect to their contact with Fas2$^+$ axon tracts (Fig. 2E,H-L). When both astrocytes were positioned dorsally (Cat.1 D/D, n=15), they consistently infiltrated a dorsal-medial zone that varied only at a single landmark fascicle [Fig. 2I,J, yellow; Cat.1a (n=9) versus Cat.1b (n=6)]. When both astrocytes were positioned laterally (Cat.2 L/L, n=19), they covered an invariant lateral territory (Fig. 2I,J, red). Finally, arbors of the dorsal and ventral pair (Cat.3 D/V, n=20) infiltrated a ventral-to-medial territory, with variability at one landmark only [Fig. 2I,J, orange; Cat.3a (n=13) versus Cat.3b (n=7)]. Thus, the data reveal a largely stereotyped astroglial map in which identifiable astrocytes (Fig. 2K) consistently infiltrate specific zones of the synaptic neuropil (Fig. 2J-L).

Lineage mapping and diversification of LG

Reproducibility among astrocytes could stem from stereotyped births and migrations within the lineage. We never observed two-cell clones pairing an astrocyte and an ensheathing glial cell, suggesting that the last divisions are symmetric. To further understand the lineage we examined *Nazgul-nGFP* by live imaging (Fig. 3A,C). At the onset of *Nazgul-nGFP* expression (0 min), four cells per hemisegment were labeled, and could be followed until embryos reached stage 16 (144 min). In that time, each of these cells divided only once. These terminal divisions did not appear tightly coordinated or sequential (Fig. 3C). By comparing cell positioning of live cells at stage 16 versus fixed and labeled cells (Fig. 3B), we conclude that the three anteriormost progenitors seen at t=0 (red, orange, yellow) give rise to three pairs of Prospero$^+$ astrocytes, whereas the

Development (2016) 143, 1170-1181 doi:10.1242/dev.133165

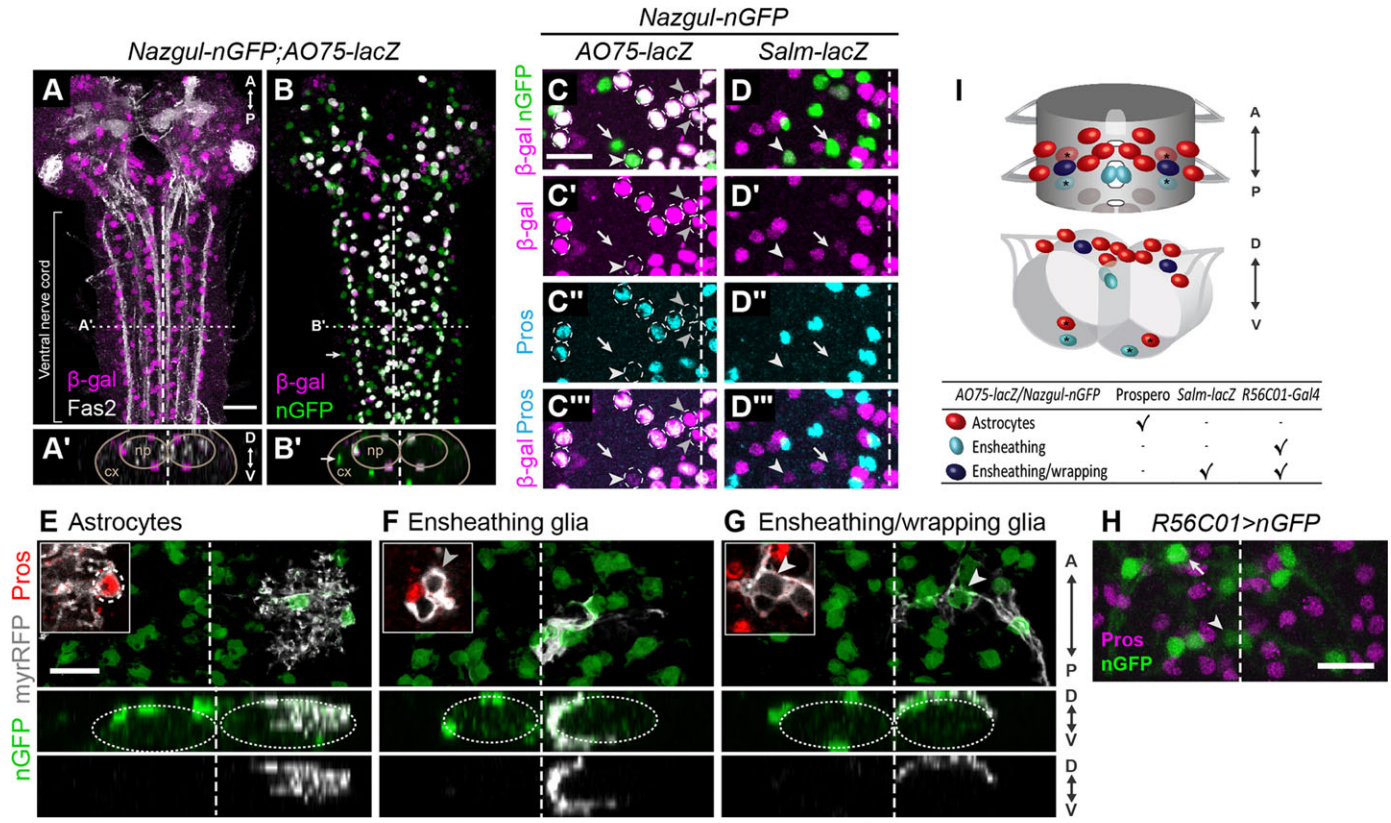

Fig. 1. Astrocytes, ensheathing glia and ensheathing/wrapping glia derive from LG. (A-B′) *Drosophila* L1 larvae longitudinal glia (LG) labeled with *AO75-lacZ* (magenta) and (A,A′) axon tracts with Fas2 (white) or (B,B′) *Nazgul-nGFP* (green), which labels LG and other glia (cortex glia, arrows). All cells expressing *AO75-lacZ* co-express *Nazgul-nGFP*. (A,B) 3D horizontal views of confocal *z*-stack, (A′,B′) transverse sections. np, neuropil; cx, cortex. (C-C‴) Among nine LG by hemisegment (AO75-*lacZ*$^{+}$, dashed circles), six express Prospero (Pros, cyan). Arrowheads indicate Prospero^{-} LG. (D-D‴) The lateral posterior LG (LP-LG) expresses *Salm-lacZ* (arrowheads). Arrows (C-D‴) show medial intersegmental nerve glia (M-ISNG) (*Nazgul-nGFP*$^{+}$ but not *AO75-lacZ*$^{+}$). (E-G) Blown-OUT clones reveal LG morphologies. LG nuclei labeled with nGFP (green) and clones with myr-RFP (white) driven by *Eaat1-Gal4*. Shown are two-cell clones of two astrocytes infiltrating the neuropil (E), or two ensheathing glia enveloping the medial and ventral neuropil (F). Single-cell clones were ensheathing/wrapping glia, covering the dorsal neuropil and the proximal part of the intersegmental nerve (G). Only astrocytes express Prospero (insets). Images are horizontal 3D reconstructions (top) or orthogonal views (bottom). (H) Non-astrocytic LG do not express Prospero. *R56C01-Gal4;UAS-nGFP* was used to specifically label ensheathing (arrowhead) and ensheathing/wrapping glia (arrow) (see Table 1). Prospero (magenta) shows no overlap with nGFP (green). Horizontal view, maximal projection of confocal *z*-stack. (I) Idealized larval ventral nerve cord (VNC) neuropil (one segment). Each hemisegment has six astrocytes, two ensheathing glia and one ensheathing/wrapping glia. Dashed line indicates the midline. Scale bars: 20 µm in A-B′; 10 µm in C-H.

posteriormost progenitor (cyan) produces the pair of ensheathing glia (Fig. 3D). The idealized view of the LGB lineage that we propose in Fig. 3D is supported by over 85% of the four-cell clones we observed, as 62.9% were composed of the Cat.1 D/D and Cat.2 L/L pairs of astrocytes, whereas 22.9% consisted of the Cat.3 D/V pair of astrocytes and the ensheathing glia pair. We could not track the origin of the LP-LG, the ninth cell of the LGB lineage, as it became newly labeled with *Nazgul-nGFP* with no visible progenitor (Fig. 3C, dark blue). The data suggest that LP-LG arises independently within the lineage and might derive from the asymmetric division of the LGB itself (Fig. 3D): (1) it was the only LG found in single-cell clones (n=13); (2) it was never found

Table 1. Gal4 drivers used in this study

Gal4 driver	Expression in LG	Expression in M-ISNG	Onset of GFP detection in LG*	References
Eaat1-Gal4	All (weaker in Prospero^{-} cells)	Weak	Stage 11	Beckervordersandforth et al., 2008; Rival et al., 2006; Rival et al., 2004; Stacey et al., 2010
Nazgul-Gal4	All	Yes	Stage 12-13	Stacey et al., 2010; this work
R25H07-Gal4	All	Stochastic	Stage 13	Jenett et al., 2012; this work
R56C01-Gal4	Ensheathing glia and ensheathing/wrapping glia	Yes	Late stage 17	Jenett et al., 2012; this work
R56F03-Gal4	Ensheathing glia and ensheathing/wrapping glia (stochastic expression in rare astrocytes)	Yes	Stage 14	Jenett et al., 2012; this work

Gal4 driver expression characterized in LG by us (*Nazgul-Gal4*, *R25H07-Gal4*, *R56C01-Gal4* and *R56F03-Gal4*) or others (*Eaat1-Gal4*) as indicated. These lines are also expressed in other cells, but are specified here only for M-ISNG.

*In this work, Gal4 lines were crossed to UAS-GFP, and dechorionated embryos were live-mounted in halocarbon oil to be assessed for GFP expression by confocal microscopy.

Development (2016) 143, 1170-1181 doi:10.1242/dev.133165

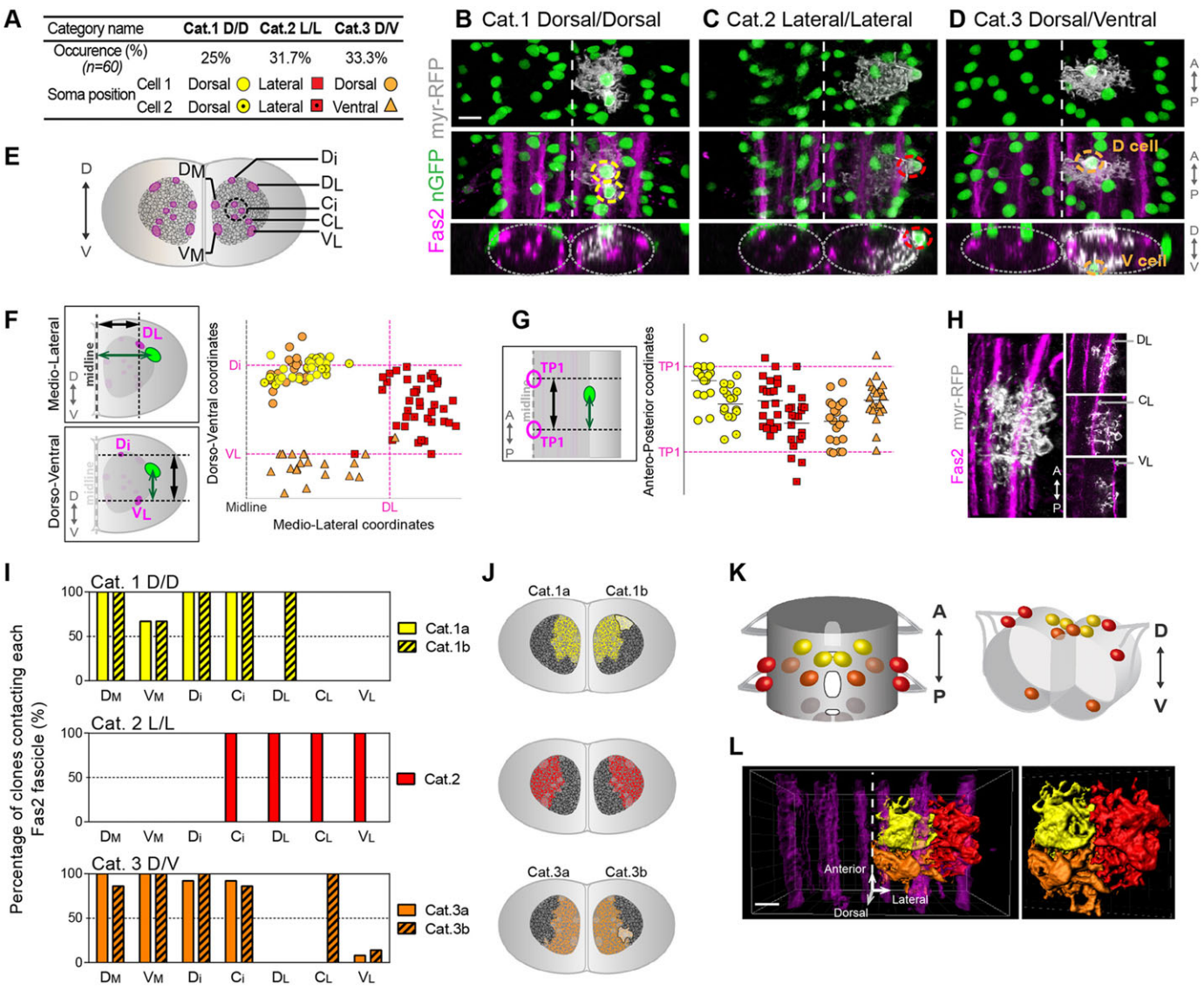

Fig. 2. Astrocytes cover stereotyped territories of the CNS neuropil. (A-G) Astrocyte cell bodies allocate to particular regions around the synaptic neuropil. (A-D) Three categories of astrocyte two-cell Blown-OUT clones obtained with the *Eaat1-Gal4* driver. (A) Classification summary and examples of clones with (B) both astrocytes dorsal to the neuropil (Cat.1 D/D), (C) both astrocytes lateral (Cat.2 L/L) or (D) one dorsal and one ventral (Cat.3 D/V). Glial nuclei labeled with nGFP (green), clones with myr-RFP (white) and axon tracts with anti-Fas2 (magenta). Dashed circles indicate astrocyte nuclei within clones. 3D reconstructions of *z*-stacks, anterior up; beneath are transverse sections, dorsal up. Dashed line indicates the midline. Scale bars: 10 µm. (E-G) Within each region, astrocyte positions are imprecise. (E) Schematic of larval VNC transverse section showing major Fas2^{+} axon bundles (magenta) used to chart two-cell astrocyte clones, named according to their dorsoventral (D, dorsal; C, central; V, ventral) and mediolateral (M, medial; i, intermedial; L, lateral) position. (F,G) Relative coordinates of each astrocyte nucleus. Charting along (F) the mediolateral and dorsoventral axes with reference to the midline and specific Fas2^{+} axon bundles or (G) the anteroposterior axis using the Fas2^{+} transverse projection 1 (TP1). In diagrams on the left: black arrows, reference distance between landmarks; green arrows, distance from nGFP-labeled nucleus to landmark. (H-L) Astrocytes reproducibly cover distinct neuropil territories. (H) Technique for charting astrocyte territories: example of a two-cell clone with arbor (myr-RFP, white) that contacts specific Fas2^{+} axon bundles (magenta). (Left) 3D reconstruction of *z*-stack; (right) single *z*-sections at levels in the neuropil. Anterior is up. (I) Contacts made by astrocytes with Fas2^{+} axon bundles in each category of two-cell clones. Results are expressed as the percentage of clones from a given category that contacted the indicated fascicles. Cat.2 L/L territories are invariant (n=19), whereas Cat.1 D/D (n=15) and Cat.3 D/V (n=20) exhibit modest variability, by which they can be subdivided further. (J) Transverse views of 2D astroglial maps illustrating our findings on how astrocytes parcel the neuropil territory (dorsal is up). (K) Idealized spatial placement of the cell bodies of each sibling pair of astrocytes in a segment. (L) 3D reconstruction model (Imaris) of six astrocytes in a hemisegment, a composite of three distinct two-cell clones. (Right) An enlarged view. Dashed line, midline. Scale bar: 30 µm.

in two-cell clones; and (3) none of the few eight-cell clones (n=3) we observed included LP-LG.

Astrocytes and ensheathing glia are distinguished by expression of Eaat1 and Eaat2

Astrocytes were shown recently to express the GABA transporter Gat (Stork et al., 2014). Previously, the glutamate recycling enzyme Glutamine synthetase 2 (Thomas and van Meyel, 2007) and the N-β-alanyl-biogenic amine synthetase Ebony (Kato et al., 2011) were shown to be expressed in Prospero^{+} glia. Also, mRNAs for *Eaat1*, the only *Drosophila* glutamate transporter (Besson et al., 2000), and *Eaat2*, a transporter for taurine and aspartate (Besson et al., 2005, 2011, 2000), were shown to be expressed in discrete subsets of glia in the embryonic CNS (Freeman et al., 2003;

Development (2016) 143, 1170-1181 doi:10.1242/dev.133165

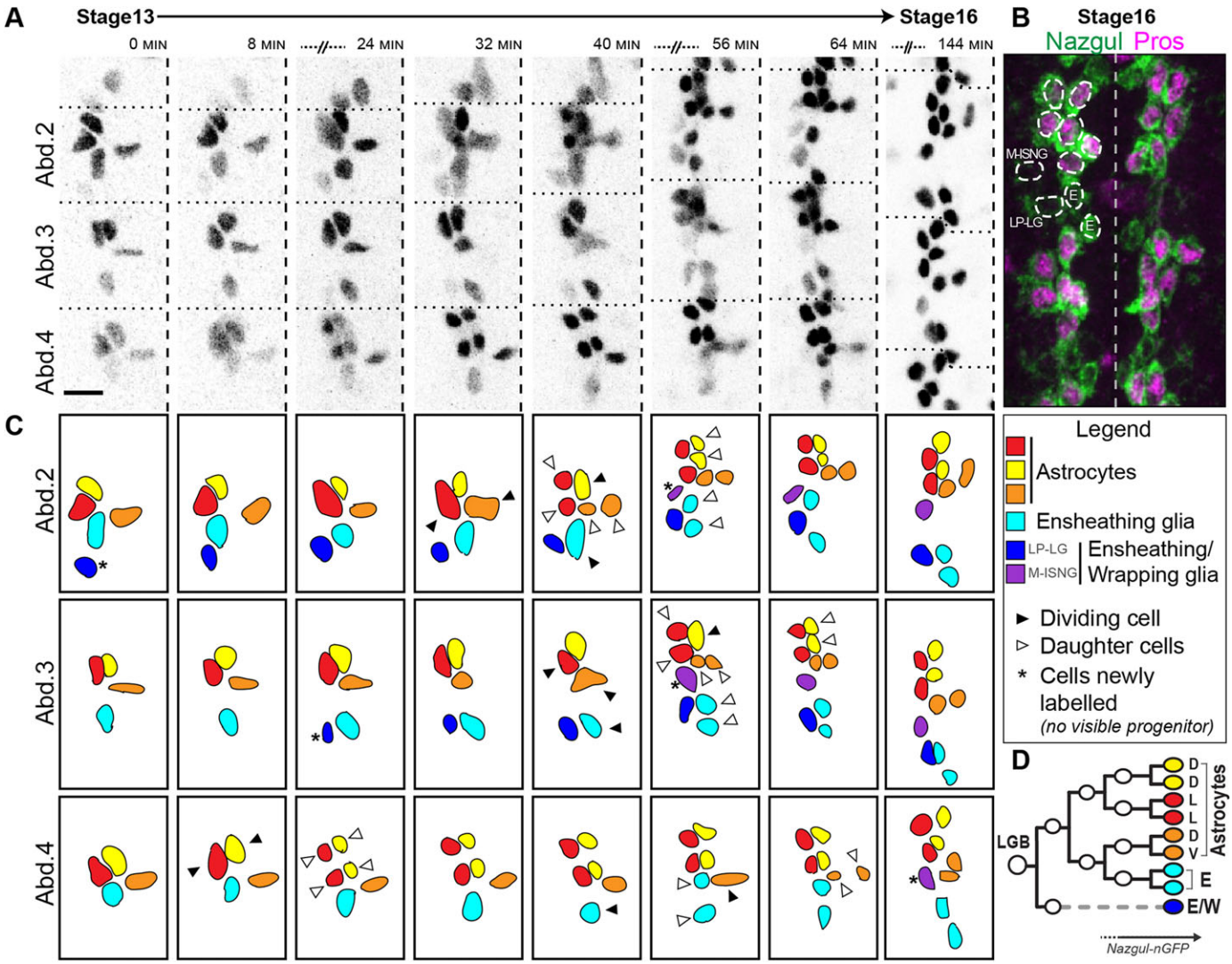

Fig. 3. Live imaging of the births of astrocytes and ensheathing glia. (A) LG visualized with *Nazgul-nGFP* at embryonic stages 13 to 16. Horizontal views of three abdominal hemisegments (Abd.2-4). Anterior is up; dashed vertical lines, midline. Time is shown in minutes, with images at selected time points. Scale bar: 10 µm. (B) Fixed VNC of a stage 16 embryo: Nazgul (green) labels nine LG and M-ISNG; Prospero (magenta) colabels in astrocytes. (C) Schematic interpretation of A. At 0 and 8 min, four cells were consistently arranged in each hemisegment and by 64 min had divided only once (black arrowheads). Through their reproducible positioning at 144 min, the mature identities of the resulting eight cells were assigned based on the cell arrangement in B. Astrocytes are in yellow (Cat.1 D/D), red (Cat.2 L/L) or orange (Cat.3 D/V) and ensheathing glia in cyan. *Nazgul-nGFP* also newly labeled one or two additional cells in each hemisegment (asterisks), corresponding to the ensheathing/wrapping glia LP-LG (blue) and M-ISNG (purple). (D) Idealized view of the longitudinal glioblast (LGB) lineage. LGB gives rise to three pairs of astrocytes, one pair of ensheathing glia (E) and a single ensheathing/wrapping glial cell (E/W).

Soustelle et al., 2002; Stacey et al., 2010). We raised antisera to Eaat1 and Eaat2, and found that the Eaat1 antibody strongly labeled astrocytic membranes (Fig. 4A-Ac). Ensheathing glia (Fig. 4, blue brackets) and ensheathing/wrapping glia (Fig. 4, arrows) express lower levels of Eaat1 (Fig. 4A-Ac) and, more notably, they express Eaat2 (Fig. 4A′-Ac′). The latter was confirmed by selective RNAi knockdown of Eaat2 from ensheathing and ensheathing/wrapping glia (Fig. 4C) using the newly characterized *R56C01-Gal4* (Fig. 4E, Table 1). Therefore, subtypes of LG are specialized for the uptake and metabolism of different neuroactive molecules (summarized in Fig. 4D,E).

Pointed P1 is required for astrogenesis

Which molecular mechanisms promote the acquisition of different glial identities? The Ets transcription factor Pointed P1 (PntP1) is specifically expressed in embryonic LG and required early for their proper differentiation (Klaes et al., 1994). But whether PntP1 selectively contributes to the programs that generate the distinct LG subtypes has not been determined. To examine this, we induced RNAi knockdown of *pointed* gene products [*PntP1* and *PntP2* (Klambt, 1993)] in all LG using *R25H07-Gal4* (Fig. 4E, Table 1). At L1, these cells were mispositioned to occupy only the dorsal perimeter of the neuropil (Fig. 5D), but they retained expression of the glial marker Repo (Fig. S1A,B,G). Remarkably, the analysis of molecular markers to distinguish astrocytes (Prospero, Ebony, Gat, Eaat1^{high}) from ensheathing glia (Eaat2, Eaat1^{low}) revealed specific impairment of astrocyte differentiation. Prospero and Ebony, which are normally co-expressed in astrocytes (Fig. 5A,A′), were lost (Fig. 5D,D′). Also lost were astrocytic processes within the neuropil labeled with a membrane-tethered GFP (Fig. 5E compared with control in Fig. 5B), Eaat1 (Fig. 5Fb,b′) or Gat (data not shown).

Interestingly, we also observed a broadening of Eaat2-expressing membranes surrounding the neuropil (Fig. 5Fa-b″, brackets) compared with controls (Fig. 5Ca-b″). This suggests that

Development (2016) 143, 1170-1181 doi:10.1242/dev.133165

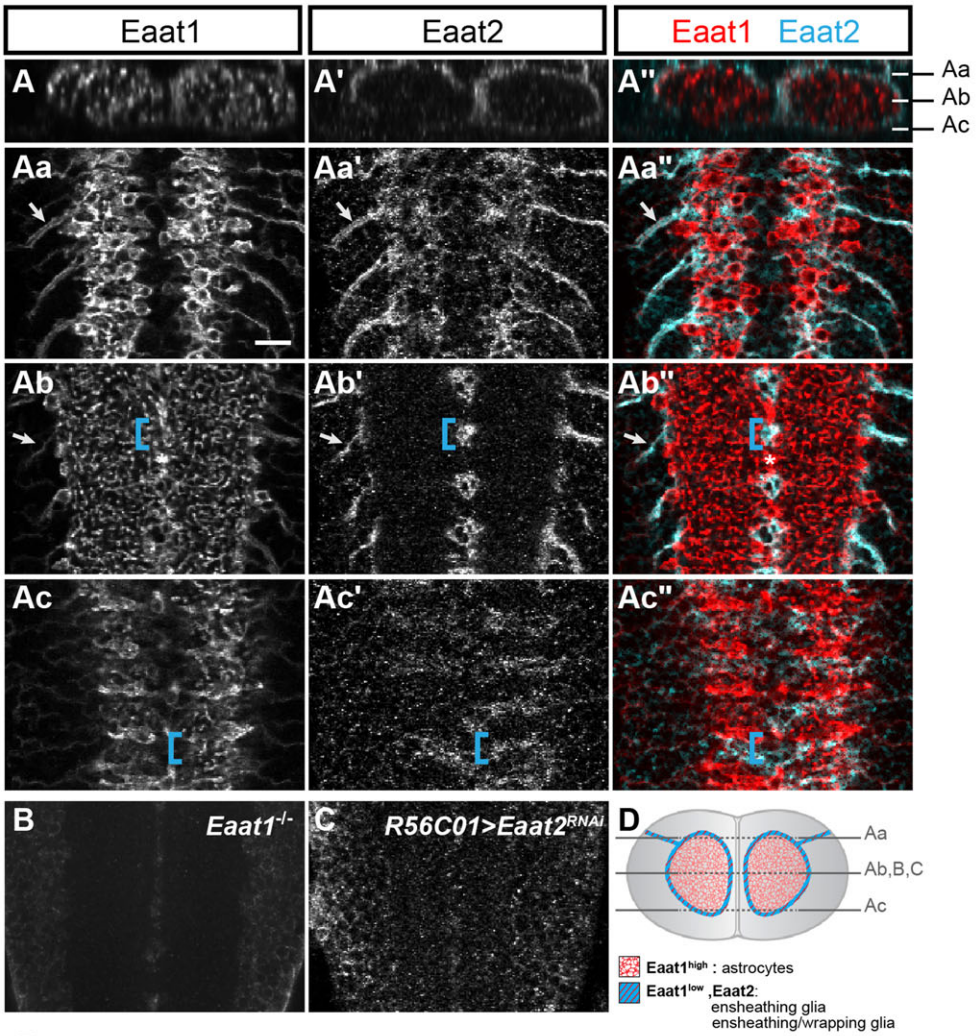

E

Tools		Astrocytes	Ensheathing	E/W	Onset in LG
Markers	Prospero	√	-	-	stage 12 *
	Ebony	√	-	-	stage 16
	Eaat1	√ high	√ low	√ low	mid/late stage 16
	Eaat2	-	√	√	mid/late stage 16
GAL4 drivers ‡	*R25H07-Gal4*	√	√	√	stage 13 §
	R56C01-Gal4	-	√	√	late stage 17 §
	R56F03-Gal4	¶	√	√	stage 14 §

. *Griffiths et al., 2007. ‡ See Table 1 for more details. § Onset of Gal4-driven *UAS-GFP* in LG. ¶ Weak and stochastic expression in rare astrocytes.

Fig. 4. Eaat1 and Eaat2 expression distinguishes LG subtypes. (A-Ac″) Colabeling for the glutamate transporter Eaat1 and the taurine/aspartate transporter Eaat2 in L1 VNC. Scale bar: 10 µm. (A-A″) Transverse images noting the focal planes of the horizontal images (Aa-c, single *z*-sections). (A-Ac) Eaat1 is expressed at high levels on astrocytic membranes, at lower levels in ensheathing glia and the ensheathing/wrapping glia LP-LG (blue brackets) and M-ISNG (arrows), and by midline glia (asterisks). (A′-Ac′) Eaat2 is restricted to ensheathing glia covering the medial and ventral neuropil between neuromeres (blue brackets) and ensheathing/wrapping glia (arrows). (A″-Ac″) Merge of Eaat1 and Eaat2. (B) Specificity of the Eaat1 antiserum confirmed by loss of Eaat1 immunoreactivity in *Eaat1* null mutants. (C) Specificity of Eaat2 antiserum confirmed by Eaat2 RNAi knockdown with *R56C01-Gal4*, a driver specific to ensheathing and ensheathing/wrapping glia. (D) Schematic summary of Eaat1 and Eaat2 expression. (E) Key molecular markers (antibodies) and Gal4 drivers used in this study.

ensheathing glia fate was not impaired by loss of Pointed, and raised the possibility that this led astrocytes to switch to an ensheathing glia fate. Similar results were obtained by overexpressing a constitutively active form of the PntP1 antagonist Anterior open (Aop^{ACT}) (Brunner et al., 1994) (Fig. S2A-D2). Our data reveal that, although all LG need PntP1 for correct positioning, PntP1 is selectively required for the terminal differentiation of astrocytes.

Notch and Prospero promote astrogenesis at the expense of ensheathing glia

The loss of astrocytes caused by the inhibition of Pointed was accompanied by loss of Prospero expression. We showed previously that Notch signaling through Fringe, a glycosyltransferase that sensitizes the Notch receptor to the Delta ligand, maintains expression of Prospero in the anteriormost six LG in stage 16 embryos (Thomas and van Meyel, 2007) and positively regulates *Eaat1* transcription (Stacey et al., 2010). To examine whether Notch regulates the astrogenic program, we overexpressed Hairless, a transcriptional repressor of the Notch pathway (Fig. 5G-Ib″). In L1 larvae, we found that this antagonism of Notch caused a severe reduction of Prospero expression but, in contrast to *pointed* RNAi, only modest alteration of cell positioning. Neither cell number nor Repo expression was affected (Fig. S1C,G), but there was a severe reduction in Ebony (Fig. 5G,G′) and, within the neuropil, losses of astrocyte infiltration ($CD4\text{-}tdGFP^{+}$ membranes, Fig. 5H), of Eaat1 (Fig. 5Ib,b′) and of Gat (data not shown). We found Eaat1-labeled membranes gathered around the neuropil instead (Fig. 5Ib,b′), accompanied by broadened expression of Eaat2 (Fig. 5Ia-b″,

Development (2016) 143, 1170-1181 doi:10.1242/dev.133165

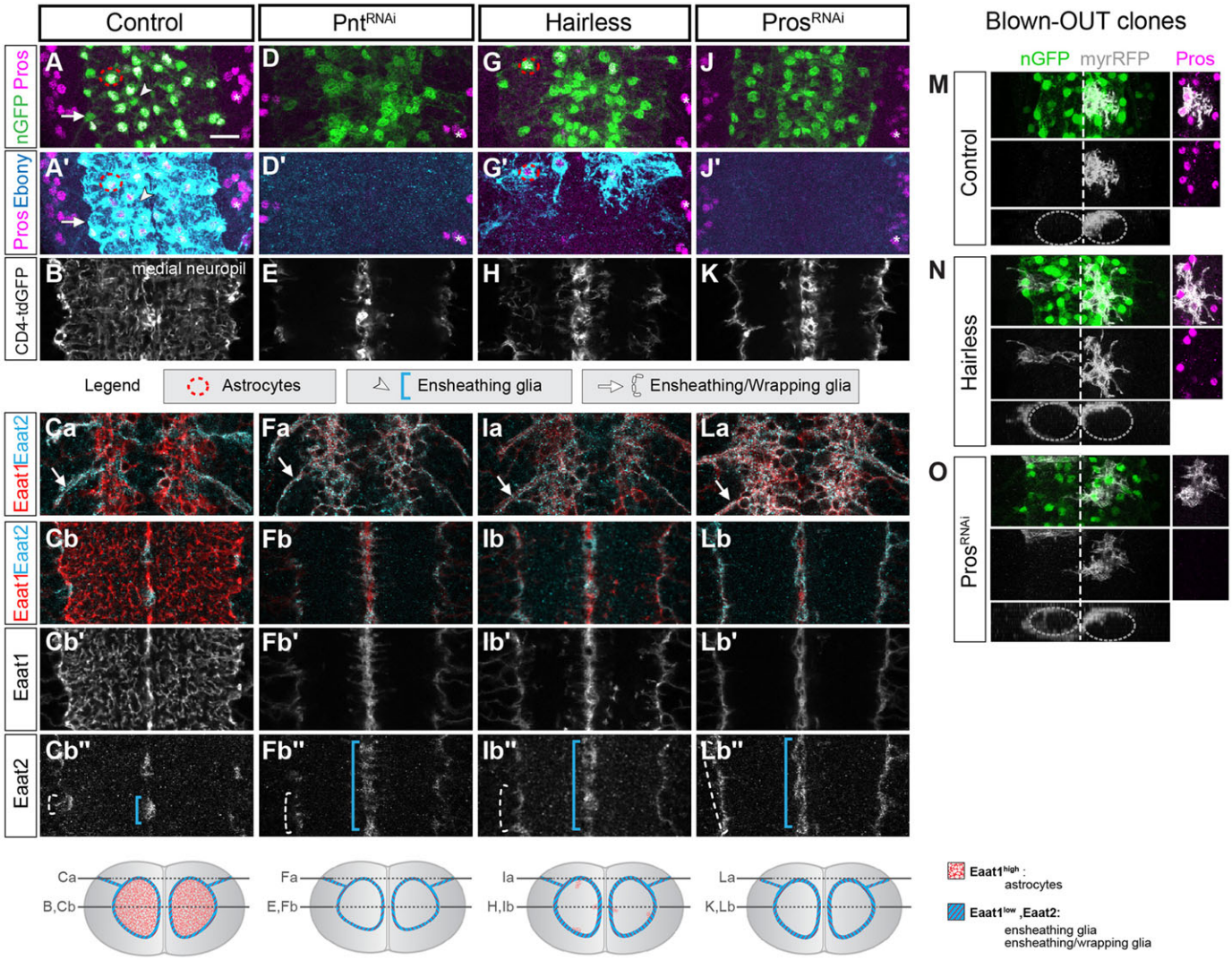

Fig. 5. Astrogenesis requires Pointed, Notch and Prospero. Representative images of L1 VNCs double labeled for (A-J′) Prospero and Ebony or for (Ca-Lb″) Eaat1 and Eaat2, and (B,E,H,K) astrocytic processes marked by CD4-tdGFP. Images are maximum projection of confocal *z*-stacks (A-J′) or single *z*-sections at the focal planes indicated at the bottom of the figure. Bottom schematics also illustrate the findings shown in Ca-Lb″. *R25H07-Gal4* was used to target all LG. (A-Cb″) A typical example of the control (*n*=15 VNCs examined). (D-Fb″) *pointed* RNAi (*n*=12). Prospero and Ebony expression is lost and LG are mispositioned (D,D′), and astrocytic processes [marked by the expression of a membrane-tethered GFP (CD4-tdGFP) shown at the medial level in the neuropil (E) or by Eaat1 (Fb,b′)] fail to infiltrate the neuropil; Eaat2 expression broadens (Fb″, bracket) and co-expression of Eaat1 and Eaat2 increases (Fa). (G-Ib″) Inhibition of Notch with Hairless (*n*=10). Loss of Prospero and Ebony in most GFP^{+} LG (G,G′). Astrocytic processes marked by CD4-tdGFP (H) or by Eaat1 (Ib,b′) seldom infiltrate the neuropil, Eaat2 labeling broadens (Ib″, bracket), and co-expression of Eaat1 and Eaat2 expands (Ia). (J-Lb″) *prospero* RNAi has effects similar to Hairless (*n*=10). Scale bar: 10 µm. (M-O) Blown-OUT analysis of Notch inhibition and Prospero knockdown by RNAi. *Nazgul-Gal4* was used to label glial cell nuclei with GFP (green), two-cell Blown-OUT clones with myr-RFP (white), and astrocytes with Prospero (magenta, right-hand column). All panels are horizontal sections (anterior is up), except bottom panel transverse views (dorsal is up). Dashed lines indicate the midline; dotted ovals outline the neuropil. (M) Control two-cell astrocyte clone (Cat.1 D/D): both cells infiltrate the neuropil and express Prospero. (N) Notch inhibition with Hairless: two pairs of two-cell clones in the positions of astrocytes fail to infiltrate the neuropil and do not express Prospero. (O) Prospero knockdown by RNAi has effects similar to Hairless: loss of Prospero and lack of neuropil infiltration.

brackets). This could result from expansion of ensheathing glia membranes upon loss of astrocytic membranes, or to the transformation of astrocytes into ensheathing glia. To distinguish between these two possibilities, we used the Blown-OUT technique to visualize individual cells overexpressing Hairless (Fig. 5N). We found that Prospero^{-} Hairless^{+} clones with cell bodies in the positions of dorsal astrocytes adopted an ensheathing-like morphology, with membranes at the interface of the neuropil and cortex (compare with control, Fig. 5M), whereas clones of ensheathing glia were unaffected (data not shown). Altogether, our data indicate that Notch signaling is required for astrocyte differentiation and that, in the absence of Notch, cells adopt an ensheathing glia-like profile at both the molecular and morphological levels.

What is the role of Prospero in this process? RNAi knockdown of Prospero itself abolished Ebony expression (Fig. 5J,J′) (Kato et al., 2011) and prevented astrocyte infiltration into the neuropil (Fig. 5K-Lb′). This was not the result of having fewer cells, since cell number and Repo expression were unaffected (Fig. S1D,G). Therefore, our results indicate that Prospero is not simply a marker for developing astrocytes, it is also essential for astrocyte differentiation. On the other hand, Prospero knockdown also

Development (2016) 143, 1170-1181 doi:10.1242/dev.133165

broadened the expression of Eaat2 along the surface of the neuropil (Fig. 5La-b″, brackets). Consistent with this, Blown-OUT clones had a flattened appearance and did not infiltrate the neuropil (Fig. 5O). This strongly supports the idea that impairment of astrocyte fate is accompanied by promotion of ensheathing glia fate.

Interplay of Pointed, Notch and Prospero in the control of astrogenesis

To assess whether Notch activation could drive ensheathing glia toward an astrocyte fate, we expressed a constitutively active form of Notch (Notch^{ICD}) in LG. Misexpression of Notch^{ICD} can drive Prospero expression in embryonic LG that do not normally express it (Griffiths and Hidalgo, 2004; Thomas and van Meyel, 2007). Here, we found that Notch^{ICD} induced not only ectopic Prospero but also ectopic Ebony (Fig. 6C,C′, arrowheads) and Gat (data not shown), and that the domain of Eaat2 expression was severely reduced, especially at medial and ventral neuropil between neuromeres, where ensheathing glia normally reside (Fig. 6Db,b″).

This evidence for an instructive role for Notch signaling in astrogenesis is supported by analysis of Blown-OUT clones expressing Notch^{ICD} (Fig. S3). In controls (n=38), 86.8% were pairs of Prospero^{+} astrocytes (Fig. S3A,A′), while 13.2% of two-cell clones were pairs of Prospero^{-} ensheathing glia (Fig. S3C,C′). Upon activation of Notch signaling with Notch^{ICD} (n=25), 96% were pairs of Prospero^{+} astrocytes (Fig. S3B-D′) and 4% were pairs of ensheathing glia – in these cases, the ensheathing glia did not express Prospero (Fig. S3D,D′, white arrowhead). Among astrocyte clones, the increase is largely in the Cat.3 D/V (13.2% in controls versus 28% in Notch^{ICD}). Similarly, in four-cell Blown-OUT clones, whereas in controls (n=28) 46.4% comprised a Cat.3 D/V astrocyte pair and two ensheathing glia, upon Notch^{ICD} expression all clones were astrocytes only. Together, these results indicate that Notch induces astrocyte differentiation at the expense of ensheathing glia. When Notch^{ICD} did not convert ensheathing glia to astrocytes, the ensheathing glia did not express Prospero (Fig. S3D, white arrowhead), signifying that Prospero might be a key effector of Notch in this process. In keeping with this, Prospero knockdown entirely mitigated the ability of Notch^{ICD} to induce ectopic astrogenesis (Fig. 6E-Fb).

Thus, both PntP1 and Notch signaling are required for Prospero expression and differentiation of astrocytes, and Notch signaling is sufficient to induce Prospero and drive astrogenesis in cells that would otherwise become ensheathing glia (Fig. 6C-Db″). We examined whether Notch^{ICD} could induce Prospero in this manner if PntP1 function were blocked by its antagonist Aop. In these conditions, animals were unable to hatch and so were examined at stage 17 of embryogenesis (Fig. 6G-Hb). We found that Notch^{ICD} could not induce Prospero or Ebony (Fig. 6G,G′) or infiltration of the neuropil (Fig. 6Hb). Therefore, *pointed* blockade renders LG incapable of becoming astrocytes in response to Notch. Since overexpression of PntP1 does not induce ectopic Prospero expression (data not shown), our data argue that the early role of PntP1 in the differentiation of LG allows Notch signaling to selectively induce Prospero in the subset that are fated to become astrocytes (Fig. 6I).

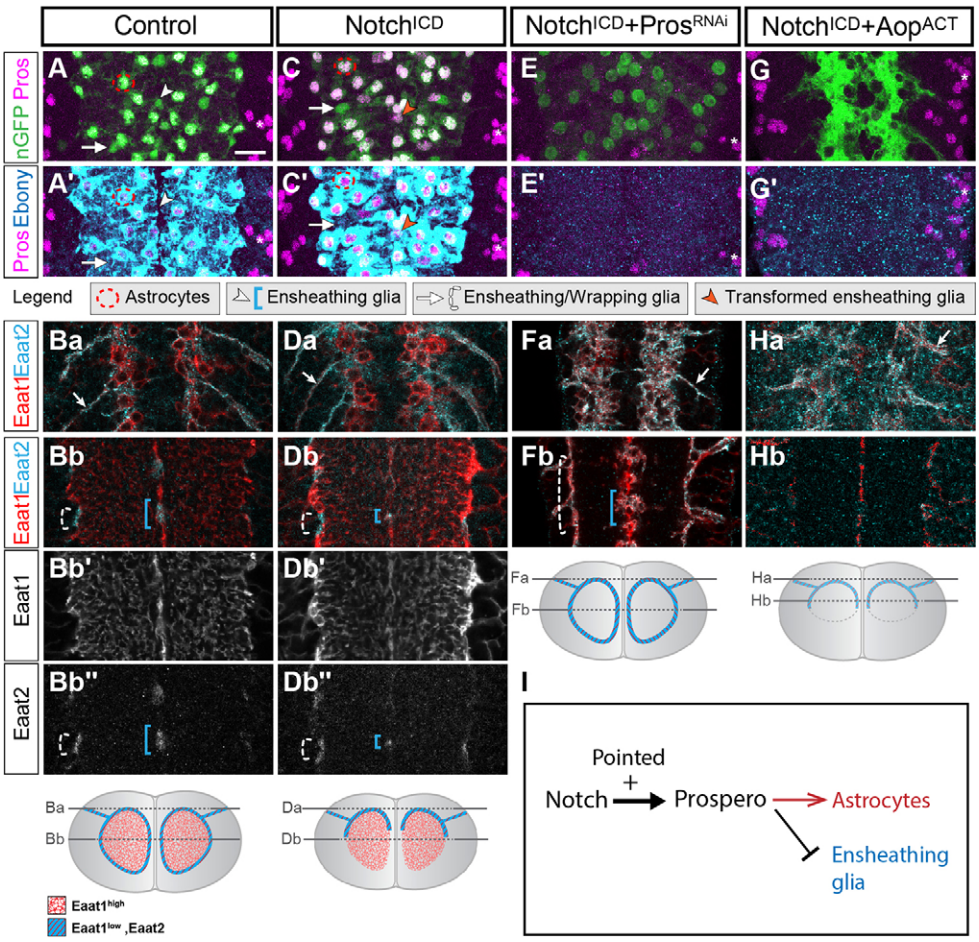

Fig. 6. Notch induction of astrogenesis requires Prospero and Pointed P1. L1 larval (A-Fb) or E17 (G-Hb) VNCs colabeled for (A-G′) Prospero and Ebony (maximum projection of *z*-stack) or (Ba-Hb) Eaat1 and Eaat2 (single *z*-section at the focal planes shown at the bottom). *R25H07-Gal4,UAS-nGFP* was used to target all LG. Schematics at the bottom also illustrate the findings of Ba-Hb. (A-Bb″) Control (n=15). (C-Db″) Activation of Notch signaling with Notch^{ICD} (n=12). Ensheathing glia are induced to express Prospero and Ebony (arrowheads in C,C′) and lose expression of Eaat2 (blue bracket in Db). Ensheathing/wrapping glia are not sensitive to Notch activation, as they do not express ectopic Prospero or Ebony (arrows in C,C′) and Eaat2 remains unaffected (arrow in Da, dashed white brackets in Db-b″). (E-Fb) Simultaneous knockdown of Prospero (n=12) blocks the astrogenic effects of Notch signaling (Ebony expression, membrane infiltration) on ensheathing glia. (G-Hb) Notch activation does not overcome the effect of Pointed P1 (PntP1) inhibition with Aop^{ACT} (n=10). Additional controls at embryo stage 17 are shown in Fig. S2. (I) Interplay of Pointed, Notch and Prospero in astrogenesis. Scale bar: 10 µm.

Development (2016) 143, 1170-1181 doi:10.1242/dev.133165

Prospero itself drives astrocyte differentiation

Others have shown that Prospero can activate glial gene expression (Choksi et al., 2006; Kato et al., 2011), and our data here suggested that Prospero might play an active role in instructing astrocytic fate. We misexpressed Prospero specifically in Prospero^{-} LG using *R56F03-Gal4* (Fig. 4E, Table 1). Remarkably, misexpression of Prospero in these cells led to ectopic expression of the astrocyte markers Ebony (Fig. 7Cb,c) and Gat (data not shown), as compared with the control (Fig. 7Aa-c), and caused these cells to grow Eaat1^{+} astrocyte-like processes into the neuropil (Fig. 7Ca,a′,D compared with control Fig. 7Aa,a′,B). This pro-astrocytic effect was accompanied by the loss of Eaat2 expression in all cells that normally express it (Fig. 7D′ versus control Fig. 7B′). We conclude that Prospero is both necessary and sufficient for astrogenesis.

DISCUSSION

We report the differentiation of *Drosophila* astrocytes from a multipotent glioblast that also gives rise to ensheathing glia. We provide new insight into the organization of the synaptic neuropil by discovering that *Drosophila* astrocytes are allocated to specific regions and cover stereotyped territories to form an astroglial map. In addition, we describe a program for astrocyte differentiation in which PntP1 allows Notch signaling to engage its key effector Prospero.

Allocation of larval astrocytes and the formation of a precise astroglial map

We have shown that *Drosophila* astrocytes are reliably allocated to consistent regions, as seen for mammalian astrocytes (Hochstim et al., 2008; Tsai et al., 2012). Molecular heterogeneity among astrocytes could account for their distinct positioning, but currently we have no evidence for it. Within these regions, astrocyte cell bodies appear imprecisely positioned and yet, to a surprising degree, their infiltrative arbors chart very precisely to particular regions of the neuropil. This specific topography of the three pairs of astrocytes delineates an astroglial map that is assembled by currently unknown means. It seems predisposed by soma position, and is surely influenced by FGF-mediated arbor ingrowth (Stork et al., 2014) and tiling, yet because soma positioning is imprecise and FGF ligands are produced broadly within the neuropil, these cannot entirely account for such precise coverage. Future research will be needed to investigate additional mechanisms that could contribute to astroglial map formation, such as targeting of astrocyte arbors via local guidance cues or the tiling of neighboring astrocytes via mutual exclusion.

In mammals, astrocytes organize into exclusive spatial domains with limited overlap with neighbors, and this topography plays a role in the function of neural networks (López-Hidalgo and Schummers, 2014). In light of this, it is intriguing that the dorsal region of the *Drosophila* VNC neuropil harbors synaptic inputs onto motor neurons and the ventral region contains synaptic inputs from sensory neurons (Grueber et al., 2007; Landgraf et al., 2003a; Merritt and Whitington, 1995; Zlatic et al., 2003). Thus, coverage of discrete territories by specific astrocytes could partition synapses in motor versus sensory neuropil, or perhaps into other functionally important subdivisions. During development, this might provide local spatial information to aid the maturation and refinement of neural circuits, and in the mature CNS this could create functionally isolated islands to provide the localized balance and coordination of ions and neurotransmitters (Halassa et al., 2007).

Astrocyte generation from a multipotent glioblast requires Pointed, Notch and Prospero

Previously, division of the LGB was shown to be followed by the medial migration of its two daughter cells to positions just dorsal to the nascent longitudinal axon tracts (Jacobs et al., 1989). Here, we provide evidence that one daughter cell gives rise to three sibling pairs of astrocytes and one pair of ensheathing glia. The other

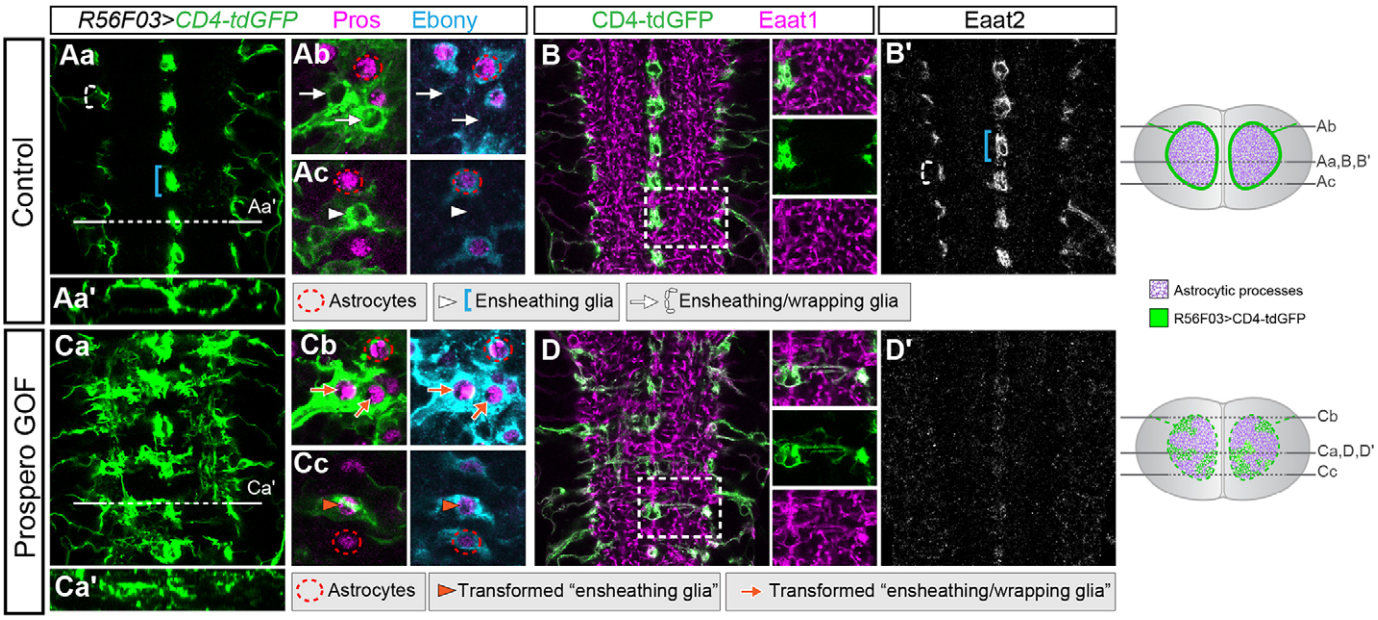

Fig. 7. Prospero is sufficient to transform ensheathing glia into astrocytes. Images are single horizontal *z*-sections; Aa′ and Ca′ are transverse views at the levels indicated in Aa and Ca. Schematics to the right summarize the findings and indicate focal planes. (Aa-B′) Control (n=15). *R56F03-Gal4* was used to drive *UAS-CD4-tdGFP* (green) to target ensheathing glia (dashed bracket in Aa; arrows in Ab) and ensheathing/wrapping glia (blue bracket in Aa; arrowheads in Ac). These cells lie flat around the neuropil (Aa,a′,B) and do not express the astrocyte markers (arrows and arrowheads in Ab,c) Prospero (magenta) or Ebony (cyan). Yet, they express Eaat2 (B′). (Ca-D′) Prospero misexpression (gain of function, GOF) (n=25) makes ensheathing glia and ensheathing/wrapping glia adopt astrocyte-like features: they express Ebony (cyan; Cb,c), their processes infiltrate the neuropil (Ca,a′,D) and they lose Eaat2 expression (D′).

Development (2016) 143, 1170-1181 doi:10.1242/dev.133165

daughter cell is likely to give rise to the ensheathing/wrapping glial cell known as LP-LG in embryos. This is notably different from the adult *Drosophila* brain, where astrocytes and ensheathing glia emerge from distinct postembryonic lineages (Awasaki et al., 2008), indicating that there are several modes of generating astrocytes in *Drosophila*.

We identified three key factors for astrocyte differentiation that are also sufficient to switch the developmental fate of LG: the Ets protein PntP1, Notch signaling and the homeoprotein Prospero. Our data support the idea that PntP1 has an early role in the differentiation of all LG (Klaes et al., 1994) and, through a mechanism that is currently unknown, it allows productive Notch signaling to selectively instruct progenitors toward the astrocyte fate. Whether this astrogenic role for Ets family factors is conserved among species remains to be explored, but it is noteworthy that glial defects in *Drosophila pointed* mutants can be rescued with vertebrate Ets1 (Albagli et al., 1996), and that Ets1 regulates the formation of radial glia in *Xenopus* (Kiyota et al., 2007).

We showed that, in the absence of Notch signaling, glial progenitors that should become astrocytes generate ensheathing glia instead. Conversely, Notch activation instructs cells that normally become ensheathing glia to acquire the morphology and molecular profile of astrocytes. These alternative glial fates are not due to the well-characterized role of Notch in asymmetric cell division, since astrocytes and ensheathing glia are born coincidentally from symmetric terminal divisions (Fig. 3). Instead, we propose they arise from Notch-dependent neuron-to-glial communication during embryogenesis. We previously found that Fringe sensitizes Notch to stimulation from developing axons bearing Delta, thus maintaining Prospero and *Eaat1* expression in a subset of LG (Stacey et al., 2010; Thomas and van Meyel, 2007). Knowing now that Prospero^{+} cells develop into astrocytes, these data support the idea that astrogenesis is promoted by neuron-to-glial Notch signaling. Astrogenesis in response to neuron-to-glial Notch signaling is likely to be conserved in mammals, where intermediate neuronal progenitors and newly born neurons express delta-like 1 (Castro et al., 2006; Namihira et al., 2009) and its obligate co-factor mindbomb 1 (Yoon et al., 2008). These have been shown, although *in vitro*, to activate Notch signaling in radial glia and to confer astroglial potential on them (Namihira et al., 2009). In this context Notch is permissive rather than instructive, as Notch-activated progenitors will only differentiate into astrocytes if they subsequently receive stimulation from gliogenic cytokines (Namihira et al., 2009).

Remarkably, we found that Prospero is a key effector of the astrogenic effect of Notch. Prospero expression is selectively maintained in newly born and mature astrocytes. Prospero is required for the differentiation of astrocytes, but not of ensheathing glia, despite their common lineage. Indeed, Prospero misexpression alone transforms ensheathing glia into astrocytes, based on a number of molecular and morphological criteria. Together, these data suggest that Prospero acts as a binary switch to distinguish astrocytes from other glial cells. Prospero orthologs exist in nematodes and mammals, and in mice they have been shown to be important for the development of a variety of organs and cell types, including neurons (Elsir et al., 2012). In vertebrates, Prospero-related homeobox 1 (Prox1) is expressed in astrocyte-like Müller cells of the retina of adult mammals and fish (Cid et al., 2010) and other glial cells (Lavado and Oliver, 2007), but whether it is involved in glial differentiation remains unknown. Interestingly, *Drosophila* glia expressing Prospero and Ebony have been shown to regenerate in response to stab injury in the larval VNC (Kato et al., 2011). Knowing now that these cells are astrocytes adds to the intriguing list of functions that *Drosophila* astrocytes share with their mammalian counterparts. Indeed, our discoveries here into how *Drosophila* astrocytes are born, how they infiltrate specific zones of the CNS neuropil, and how they differentiate in response to a specific astrogenic program will undoubtedly strengthen their utility as model system with which to study fundamental aspects of astrocyte biology and astrocyte-neuron interactions.

MATERIALS AND METHODS

Fly stocks and genetics

Drosophila melanogaster stocks were obtained from the Bloomington Stock Center [*UAS-Prospero*, *UAS-PointedP1*, *UAS-aop.ACT*, *P{PZ}salm*^{03602}, *UAS-RNAi*^{TRIP} for *PntP1* (*HMS01452*), *UAS-CD4-tdGFP*, *P{GMR25H07-Gal4}*, *P{GMR56C01-Gal4}* and *P{GMR56F03-Gal4}*]; the Vienna *Drosophila* Resource Center [*UAS-RNAi* for *prospero* (transformant ID 101477) and *Eaat2* (transformant ID 104371)]; and published sources [*UAS-Notch*^{ICD} (Go et al., 1998), *UAS-Hairless* (Maier et al., 1999), *Eaat1-Gal4* (Rival et al., 2004), *AO75-lacZ* (Beckervordersandforth et al., 2008), *20XUASB3RT>dSTOP-B3RT>myr::RFP* (Nern et al., 2011)]. We previously reported *CG31235-nGFP* and *CG31235-Gal4*, here renamed *Nazgul-nGFP* and *Nazgul-Gal4*, and null mutants for *Eaat1* (*Eaat1*$^{SM2/SM2}$) (Stacey et al., 2010).

For all RNAi experiments, control animals carried a Gal4 driver and a fluorescent reporter (i.e. *UAS-nls-GFP*). For experimental groups, we added a single copy of the RNAi construct.

Immunohistochemistry and imaging

Late embryos and L1 larvae were dissected and prepared as described previously (Stacey et al., 2010), but for anti-Eaat1 and anti-Eaat2 the tissues were treated with Bouin's fixative (Polysciences) for 10 min at room temperature. Developmental Studies Hybridoma Bank monoclonal antibodies were mouse anti-Prospero (MR1A; 1:100), mouse anti-Discs large (Dlg) (4F3; 1:200), mouse anti-Repo (8D12; 1:10) and mouse anti-Fasciclin 2 (Fas2) (1D4; 1:200). Other antibodies were rabbit: anti-β-galactosidase (β-gal) (1:1000; MP Biomedicals, 0855976), anti-Nazgul (1:500; von Hilchen et al., 2010), anti-DsRed (1:1000; Clontech, 632496), anti-Ebony (1:500; Sean Carroll, University of Wisconsin, Madison), anti-Gat (1:2000; Stork et al., 2014) and anti-Eaat1 (1:5000); guinea pig anti-Eaat2 (1:5000). Goat secondary antibodies were Alexa Fluor 647 anti-rabbit (A21244) and anti-mouse (A21235) from Molecular Probes, and Dylight594 anti-rabbit (115-517-003), Rhodamine Red-X anti-mouse (115-295-146) or anti-rabbit (111-295-144), anti-guinea pig Alexa Fluor 647 (106-605-003) or DyLight549 (106-506-003) from Jackson ImmunoResearch. Samples were mounted in SlowFade Gold reagent (Molecular Probes). Fluorescence images were acquired with an Olympus Fluoview FV1000/BX-63 confocal laser scanning microscope and processed using Fiji and Imaris (Bitplane). 3D reconstructions were generated with the Fiji 3D Viewer plug-in.

To quantify GFP^{+}/Repo^{+} cells, the total number within four adjacent abdominal segments (from among A1-A7) was divided by four, for each of five animals for every genotype.

Generation of Blown-OUT clones

Dr Tzumin Lee (HHMI, Janelia Research Campus) generously provided an unpublished stock carrying heat shock-inducible B3 recombinase (*hs-B3*) at *attP18*. Virgin *hs-B3* females were crossed to males that were either *w*$^{-}$*; Eaat1-Gal4,UAS-nls-GFP;20XUAS-B3RT>dSTOP-B3RT>myr::RFP(attP2)* or *Nazgul-Gal4,UAS-nGFP;20XUAS-B3RT>dSTOP-B3RT>myr::RFP (attP2)*. Mating adults were moved to grape juice agar plates for 12 h at 25°C, and L1 larvae were selected 0-2 h post-hatching and raised on fresh plates at 25°C until analysis 12 h afterward. No heat shock was applied as there was sufficient B3 expression to generate clones. For Blown-OUT clones expressing Hairless, *prospero* RNAi or Notch^{ICD}, males of genotype *20XUAS-B3RT>dSTOP-B3RT>myr::RFP(attP40); R25H07-Gal4,UAS-nGFP* were crossed to virgin females that were

Development (2016) 143, 1170-1181 doi:10.1242/dev.133165

either *hsB3;UAS-Hairless*, *hsB3;UAS-ProsperoRNAi* or *hsB3;;UAS-Notch^{ICD}*. For better efficiency of Gal4-UAS, grape plates containing mating adults were maintained at 29°C until analysis.

Live imaging

Nazgul-nGFP embryos were collected for 3 h and aged for 5 h at 25°C, dechorionated manually, positioned on a gas-permeable slide plate (Coy Lab Products) with ventral side up, mounted in halocarbon oil 27 (Sigma) under a coverslip and imaged on an Olympus Fluoview FV1000/BX-63 confocal microscope every 8 min using a dry 20× objective from stage 13 to 16.

Charting astrocytes and their territories

The positions of astrocytes around the neuropil were mapped relative to reference landmarks stained with anti-Fas2 (Landgraf et al., 2003b). On each axis, the distance between these reference landmarks was normalized to 1, and then the nucleus of each astrocyte was plotted in relation to that distance. Landmarks for the dorsoventral axis were the fascicles D_i and V_L. For the mediolateral axis they were the CNS midline and fascicle D_L. For the anteroposterior axis they were the transverse projection 1 (TP1) in adjacent segments. To chart the territories covered by astrocytes within the CNS neuropil, we cataloged their contacts with each one of seven identifiable $Fas2^+$ fascicles.

Eaat1 and Eaat2 antibody production

Sequences encoding the extracellular loop of Eaat1 (amino acids 117-195 of Eaat1-PA) or Eaat2 (amino acids 131-226 of Eaat2-PA) were cloned into pGEX to produce N-terminal GST fusion proteins that were IPTG-inducible (0.2 mM) in BL21 cells (Invitrogen). GST-Eaat1 and GST-Eaat2 were purified using standard procedures for insoluble proteins (Rebay and Fehon, 2009). Purified GST-Eaat1 (1 µg/µl) was injected into rabbits and GST-Eaat2 (0.5 µg/µl) into guinea pigs. Sera were tested by immunolabeling on dissected CNS tissues from control animals, null mutants for *Eaat1*, and RNAi knockdown for *Eaat2*.

Acknowledgements

We thank Tiago Ferreira for technical assistance; Marzieh Ghiasi for help in graphic design; and Yong Rao, Frieder Schöck, Jonathan Enriquez, members of the D.J.v.M. laboratory, and especially Keith Murai for advice. For fly stocks and antibodies, we thank Tzumin Lee, Ben Altenhein, Gerd Technau, Christian Klämbt, Mark Freeman, Tobias Stork, Sean Carroll, the Bloomington Stock Center and the Developmental Studies Hybridoma Bank.

Competing interests

The authors declare no competing or financial interests.

Author contributions

E.P., M.L. and D.J.v.M. conceived the study; E.P., S.D. and S.M.S. performed experiments; E.P., S.D., D.C. and D.J.v.M. analyzed the data; E.P. and D.J.v.M. wrote the manuscript; all authors approved the manuscript.

Funding

This work was supported by grants from the Canadian Institutes of Health Research (CIHR) and the Canada Foundation for Innovation (CFI) to D.J.v.M.; by a Biotechnology and Biological Sciences Research Council (UK) grant [BB/I022414/1] to M.L.; and by studentship awards to S.D. from McGill University (Max Stern) and the Integrated Program in Neuroscience.

Supplementary information

Supplementary information available online at
http://dev.biologists.org/lookup/suppl/doi:10.1242/dev.133165/-/DC1

References

Albagli, O., Klaes, A., Ferreira, E., Leprince, D. and Klämbt, C. (1996). Function of ets genes is conserved between vertebrates and Drosophila. *Mech. Dev.* **59**, 29-40.

Awasaki, T., Lai, S.-L., Ito, K. and Lee, T. (2008). Organization and postembryonic development of glial cells in the adult central brain of Drosophila. *J. Neurosci.* **28**, 13742-13753.

Barnabé-Heider, F., Wasylnka, J. A., Fernandes, K. J. L., Porsche, C., Sendtner, M., Kaplan, D. R. and Miller, F. D. (2005). Evidence that embryonic neurons regulate the onset of cortical gliogenesis via cardiotrophin-1. *Neuron* **48**, 253-265.

Beckervordersandforth, R. M., Rickert, C., Altenhein, B. and Technau, G. M. (2008). Subtypes of glial cells in the Drosophila embryonic ventral nerve cord as related to lineage and gene expression. *Mech. Dev.* **125**, 542-557.

Besson, M.-T., Soustelle, L. and Birman, S. (2000). Selective high-affinity transport of aspartate by a Drosophila homologue of the excitatory amino-acid transporters. *Curr. Biol.* **10**, 207-210.

Besson, M. T., Re, D. B., Moulin, M. and Birman, S. (2005). High affinity transport of taurine by the Drosophila aspartate transporter dEAAT2. *J. Biol. Chem.* **280**, 6621-6626.

Besson, M. T., Sinakevitch, I., Melon, C., Iché-Torres, M. and Birman, S. (2011). Involvement of the drosophila taurine/aspartate transporter dEAAT2 in selective olfactory and gustatory perceptions. *J. Comp. Neurol.* **519**, 2734-2757.

Brunner, D., Dücker, K., Oellers, N., Hafen, E., Scholz, H. and Klambt, C. (1994). The ETS domain protein pointed-P2 is a target of MAP kinase in the sevenless signal transduction pathway. *Nature* **370**, 386-389.

Bushong, E. A., Martone, M. E. and Ellisman, M. H. (2004). Maturation of astrocyte morphology and the establishment of astrocyte domains during postnatal hippocampal development. *Int. J. Dev. Neurosci.* **22**, 73-86.

Castro, D. S., Skowronska-Krawczyk, D., Armant, O., Donaldson, I. J., Parras, C., Hunt, C., Critchley, J. A., Nguyen, L., Gossler, A., Göttgens, B. et al. (2006). Proneural bHLH and Brn proteins coregulate a neurogenic program through cooperative binding to a conserved DNA motif. *Dev. Cell* **11**, 831-844.

Choksi, S. P., Southall, T. D., Bossing, T., Edoff, K., de Wit, E., Fischer, B. E., van Steensel, B., Micklem, G. and Brand, A. H. (2006). Prospero acts as a binary switch between self-renewal and differentiation in Drosophila neural stem cells. *Dev. Cell* **11**, 775-789.

Cid, E., Santos-Ledo, A., Parrilla-Monge, M., Lillo, C., Arévalo, R., Lara, J. M., Aijón, J. and Velasco, A. (2010). Prox1 expression in rod precursors and Müller cells. *Exp. Eye Res.* **90**, 267-276.

Clarke, L. E. and Barres, B. A. (2013). Emerging roles of astrocytes in neural circuit development. *Nat. Rev. Neurosci.* **14**, 311-321.

Deneen, B., Ho, R., Lukaszewicz, A., Hochstim, C. J., Gronostajski, R. M. and Anderson, D. J. (2006). The transcription factor NFIA controls the onset of gliogenesis in the developing spinal cord. *Neuron* **52**, 953-968.

Distler, C., Dreher, Z. and Stone, J. (1991). Contact spacing among astrocytes in the central nervous system: an hypothesis of their structural role. *Glia* **4**, 484-494.

Doherty, J., Logan, M. A., Tasdemir, O. E. and Freeman, M. R. (2009). Ensheathing glia function as phagocytes in the adult Drosophila brain. *J. Neurosci.* **29**, 4768-4781.

Elsir, T., Smits, A., Lindström, M. S. and Nistér, M. (2012). Transcription factor PROX1: its role in development and cancer. *Cancer Metastasis Rev.* **31**, 793-805.

Freeman, M. R., Delrow, J., Kim, J., Johnson, E. and Doe, C. Q. (2003). Unwrapping glial biology: Gcm target genes regulating glial development, diversification, and function. *Neuron* **38**, 567-580.

Go, M. J., Eastman, D. S. and Artavanis-Tsakonas, S. (1998). Cell proliferation control by Notch signaling in Drosophila development. *Development* **125**, 2031-2040.

Griffiths, R. L. and Hidalgo, A. (2004). Prospero maintains the mitotic potential of glial precursors enabling them to respond to neurons. *EMBO J.* **23**, 2440-2450.

Griffiths, R. C., Benito-Sipos, J., Fenton, J. C., Torroja, L. and Hidalgo, L. (2007). Two distinct mechanisms segregate Prospero in the longitudinal glia underlying the timing of interactions with axons. *Neuron Glia Biol.* **3**, 75-88.

Grueber, W. B., Ye, B., Yang, C.-H., Younger, S., Borden, K., Jan, L. Y. and Jan, Y.-N. (2007). Projections of Drosophila multidendritic neurons in the central nervous system: links with peripheral dendrite morphology. *Development* **134**, 55-64.

Halassa, M. M., Fellin, T., Takano, H., Dong, J.-H. and Haydon, P. G. (2007). Synaptic islands defined by the territory of a single astrocyte. *J. Neurosci.* **27**, 6473-6477.

Hochstim, C., Deneen, B., Lukaszewicz, A., Zhou, Q. and Anderson, D. J. (2008). Identification of positionally distinct astrocyte subtypes whose identities are specified by a homeodomain code. *Cell* **133**, 510-522.

Ito, K., Urban, J. and Technau, G. M. (1995). Distribution, classification, and development of Drosophila glial cells in the late embryonic and early larval ventral nerve cord. *Roux's Arch. Dev. Biol.* **204**, 284-307.

Jacobs, J. R., Hiromi, Y., Patel, N. H. and Goodman, C. S. (1989). Lineage, migration, and morphogenesis of longitudinal glia in the Drosophila CNS as revealed by a molecular lineage marker. *Neuron* **2**, 1625-1631.

Jenett, A., Rubin, G. M., Ngo, T.-T., Shepherd, D., Murphy, C., Dionne, H., Pfeiffer, B. D., Cavallaro, A., Hall, D., Jeter, J. et al. (2012). A GAL4-driver line resource for Drosophila neurobiology. *Cell Rep.* **2**, 991-1001.

Kamakura, S., Oishi, K., Yoshimatsu, T., Nakafuku, M., Masuyama, N. and Gotoh, Y. (2004). Hes binding to STAT3 mediates crosstalk between Notch and JAK–STAT signalling. *Nat. Cell Biol.* **6**, 547-554.

Kanski, R., van Strien, M. E., van Tijn, P. and Hol, E. M. (2014). A star is born: new insights into the mechanism of astrogenesis. *Cell. Mol. Life Sci.* **71**, 433-447.

Kato, K., Forero, M. G., Fenton, J. C. and Hidalgo, A. (2011). The glial regenerative response to central nervous system injury is enabled by pros-notch and pros-NFkappaB feedback. *PLoS Biol.* **9**, e1001133.

Development (2016) 143, 1170-1181 doi:10.1242/dev.133165

Kiyota, T., Kato, A. and Kato, Y. (2007). Ets-1 regulates radial glia formation during vertebrate embryogenesis. *Organogenesis* **3**, 93-101.

Klaes, A., Menne, T., Stollewerk, A., Scholz, H. and Klämbt, C. (1994). The ETS transcription factors encoded by the Drosophila gene pointed direct glial cell differentiation in the embryonic CNS. *Cell* **78**, 149-160.

Klambt, C. (1993). The Drosophila gene *pointed* encodes two ETS-like proteins which are involved in the development of the midline glial cells. *Development* **117**, 163-176.

Landgraf, M., Jeffrey, V., Fujioka, M., Jaynes, J. B. and Bate, M. (2003a). Embryonic origins of a motor system: motor dendrites form a myotopic map in Drosophila. *PLoS Biol.* **1**, e41.

Landgraf, M., Sánchez-Soriano, N., Technau, G. M., Urban, J. and Prokop, A. (2003b). Charting the Drosophila neuropile: a strategy for the standardised characterisation of genetically amenable neurites. *Dev. Biol.* **260**, 207-225.

Lavado, A. and Oliver, G. (2007). Prox1 expression patterns in the developing and adult murine brain. *Dev. Dyn.* **236**, 518-524.

Liu, H., Zhou, B., Yan, W., Lei, Z., Zhao, X., Zhang, K. and Guo, A. (2014). Astrocyte-like glial cells physiologically regulate olfactory processing through the modification of ORN-PN synaptic strength in Drosophila. *Eur. J. Neurosci.* **40**, 2744-2754.

López-Hidalgo, M. and Schummers, J. (2014). Cortical maps: a role for astrocytes? *Curr. Opin. Neurobiol.* **24**, 176-189.

Maier, D., Nagel, A. C., Johannes, B. and Preiss, A. (1999). Subcellular localization of Hairless protein shows a major focus of activity within the nucleus *Mech. Dev.* **89**, 195-199.

Merritt, D. J. and Whitington, P. M. (1995). Central projections of sensory neurons in the Drosophila embryo correlate with sensory modality, soma position, and proneural gene function. *J. Neurosci.* **15**, 1755-1767.

Molofsky, A. V., Krencik, R., Ullian, E. M., Tsai, H.-h., Deneen, B., Richardson, W. D., Barres, B. A. and Rowitch, D. H. (2012). Astrocytes and disease: a neurodevelopmental perspective. *Genes Dev.* **26**, 891-907.

Molofsky, A. V., Kelley, K. W., Tsai, H.-H., Redmond, S. A., Chang, S. M., Madireddy, L., Chan, J. R., Baranzini, S. E., Ullian, E. M. and Rowitch, D. H. (2014). Astrocyte-encoded positional cues maintain sensorimotor circuit integrity. *Nature* **509**, 189-194.

Muthukumar, A. K., Stork, T. and Freeman, M. R. (2014). Activity-dependent regulation of astrocyte GAT levels during synaptogenesis. *Nat. Neurosci.* **17**, 1340-1350.

Namihira, M., Kohyama, J., Semi, K., Sanosaka, T., Deneen, B., Taga, T. and Nakashima, K. (2009). Committed neuronal precursors confer astrocytic potential on residual neural precursor cells. *Dev. Cell* **16**, 245-255.

Nern, A., Pfeiffer, B. D., Svoboda, K. and Rubin, G. M. (2011). Multiple new site-specific recombinases for use in manipulating animal genomes. *Proc. Natl. Acad. Sci. USA* **108**, 14198-14203.

Ogata, K. and Kosaka, T. (2002). Structural and quantitative analysis of astrocytes in the mouse hippocampus. *Neuroscience* **113**, 221-233.

Omoto, J. J., Yogi, P. and Hartenstein, V. (2015). Origin and development of neuropil glia of the Drosophila larval and adult brain: Two distinct glial populations derived from separate progenitors. *Dev. Biol.* **404**, 2-20.

Rebay, I. and Fehon, R. G. (2009). Preparation of insoluble GST fusion proteins. *Cold Spring Harb. Protoc.* **2009**, pdb.prot4997.

Rival, T., Soustelle, L., Strambi, C., Besson, M. T., Iché, M. and Birman, S. (2004). Decreasing glutamate buffering capacity triggers oxidative stress and neuropil degeneration in the Drosophila brain. *Curr. Biol.* **14**, 599-605.

Rival, T., Soustelle, L., Cattaert, D., Strambi, C., Iché, M. and Birman, S. (2006). Physiological requirement for the glutamate transporter dEAAT1 at the adult Drosophila neuromuscular junction. *J. Neurobiol.* **66**, 1061-1074.

Schmid, A., Chiba, A. and Doe, C. Q. (1999). Clonal analysis of Drosophila embryonic neuroblasts: neural cell types, axon projections and muscle targets. *Development* **126**, 4653-4689.

Soustelle, L., Besson, M.-T., Rival, T. and Birman, S. (2002). Terminal glial differentiation involves regulated expression of the excitatory amino acid transporters in the Drosophila embryonic CNS. *Dev. Biol.* **248**, 294-306.

Stacey, S. M., Muraro, N. I., Peco, E., Labbe, A., Thomas, G. B., Baines, R. A. and van Meyel, D. J. (2010). Drosophila glial glutamate transporter Eaat1 is regulated by fringe-mediated notch signaling and is essential for larval locomotion. *J. Neurosci.* **30**, 14446-14457.

Stork, T., Sheehan, A., Tasdemir-Yilmaz, O. E. and Freeman, M. R. (2014). Neuron-glia interactions through the Heartless FGF receptor signaling pathway mediate morphogenesis of Drosophila astrocytes. *Neuron* **83**, 388-403.

Thomas, G. B. and van Meyel, D. J. (2007). The glycosyltransferase Fringe promotes Delta-Notch signaling between neurons and glia, and is required for subtype-specific glial gene expression. *Development* **134**, 591-600.

Tsai, H.-H., Li, H., Fuentealba, L. C., Molofsky, A. V., Taveira-Marques, R., Zhuang, H., Tenney, A., Murnen, A. T., Fancy, S. P. J., Merkle, F. et al. (2012). Regional astrocyte allocation regulates CNS synaptogenesis and repair. *Science* **337**, 358-362.

Vaessin, H., Grell, E., Wolff, E., Bier, E., Jan, L. Y. and Jan, Y. N. (1991). prospero is expressed in neuronal precursors and encodes a nuclear protein that is involved in the control of axonal outgrowth in Drosophila. *Cell* **67**, 941-953.

von Hilchen, C. M., Hein, I., Technau, G. M. and Altenhein, B. (2010). Netrins guide migration of distinct glial cells in the Drosophila embryo. *Development* **137**, 1251-1262.

Yoon, K.-J., Koo, B.-K., Im, S.-K., Jeong, H.-W., Ghim, J., Kwon, M.-c., Moon, J.-S., Miyata, T. and Kong, Y.-Y. (2008). Mind bomb 1-expressing intermediate progenitors generate notch signaling to maintain radial glial cells. *Neuron* **58**, 519-531.

Zlatic, M., Landgraf, M. and Bate, M. (2003). Genetic specification of axonal arbors: atonal regulates robo3 to position terminal branches in the Drosophila nervous system. *Neuron* **37**, 41-51.